A Dual Six-Port Automatic Network Analyzer Incorporating a Biphase-Bimodulation Element

SUNIL R. JUDAH, MEMBER, IEEE, AND ANDREW S. WRIGHT

Abstract —**Current state-of-the-art dual six-port automatic network analyzers (ANA's) are dependent upon mechanical phase shifters and attenuators. Slow measurement and calibration are among the factors that have prevented six-port ANA's from more general use outside standards and research laboratories. This paper introduces biphase bimodulation, a new technique which removes the requirement for mechanical phase shifters or attenuators. A significant increase in measurement speed is achieved, allowing quasi-real-time evaluation of scattering parameters.**

I. Introduction

IN THE EARLY 1970's, Engen [1] and Hoer [2] developed single and dual six-port network analyzers. These instruments were built with great care, and measurement of scattering parameters to great accuracy has been achieved [3]. However these dual six-port ANA systems have been dependent upon mechanical phase shifters or attenuators for successful operation.

Fig. 1 depicts the schematic diagram of a conventional dual six-port automatic network analyzer (DSPANA); computer control of the mechanical phase shifter/attenuators is not desirable for automatic implementation. The subsequent operation is slow due to the maximum switching speed of these mechanical devices (typically tens of hertz) and synchronized data collection. Although they are faster, p-i-n diode phase shifters and attenuators still require computer control and synchronized data collection. Dual six-port network analysis techniques do exhibit a performance comparable to that of heterodyne network analyzers, but at a much reduced hardware cost.

This paper introduces the concept of biphase bimodulation, which eliminates the requirement for mechanical phase shifters or attenuators. As a consequence, measurement speed is evaluated with respect to that required for quasi-real-time operation.

II. Overview

Fig. 2 illustrates a dual six-port ANA which incorporates a biphase-bimodulation element [4]. This system departs from conventional designs; the mechanical phase shifters and attenuators have been removed and replaced by the biphase-bimodulation element. A biphase-bimodulation element consists of a simple power divider, two p-i-n diode modulators, and a 3 dB quadrature coupler. This combination of microwave components accounts for the term *biphase bimodulation* [4] since during operation two audio tones are impressed upon the microwave carrier components that exhibit two different phase delays.

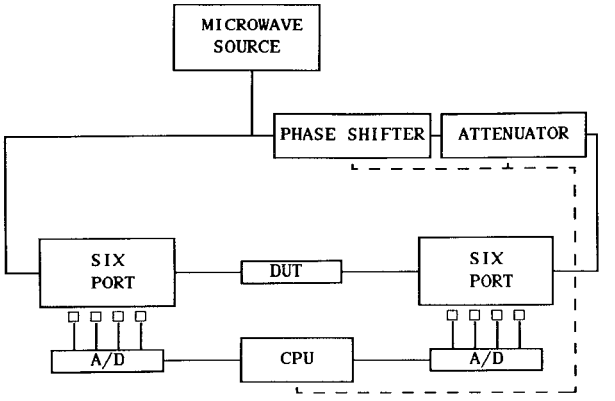

Fig. 1. A conventional dual six-port ANA.

The biphase-bimodulation element introduces a microwave carrier to the DSPANA that consists of two components. For the LHS six-port, the microwave carrier consists of a 0° phase shift labeled with the audio tone f_1 and a 90° phase shift carrier component labeled with the audio tone f_2. For the RHS six-port, the converse is true and it consists of a 0° phase shift microwave carrier component labeled f_2 and a 90° phase shift microwave carrier component labeled with the audio tone f_1.

Labeling of the microwave carrier components introduces a degree of independency that allows the system to be considered as two individual dual six-port network analyzers. The biphase information generates an effective change of state (identical to that induced by the mechanical phase shifters and attenuators of conventional six-port analyzers).

The detection system monitors the magnitude of the incident microwave energy at the detector ports of each six-port. Due to the audio tones that label the constituent microwave carrier components, Schottky barrier diode detectors are employed to demodulate the incident waveform. Active high-Q audio filters augment the detection

Manuscript received April 3, 1989; revised October 13, 1989. This work was supported by the Science and Engineering Research Council (UK) and by the Royal Signals and Radar Establishment, Marconi Instruments Ltd, Taconic Plastics Ltd, Shawinigan Research and Technology Ltd, and Densitron Ltd.

The authors are with the Department of Electronic Engineering, University of Hull, Cottingham Road, Hull, HU6 7RX, United Kingdom.

IEEE Log Number 8932994.

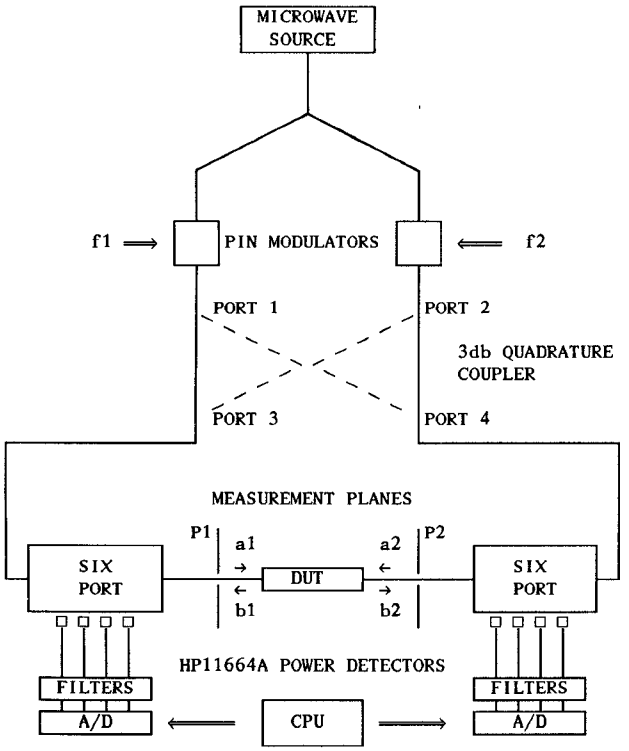

Fig. 2. Dual six-port ANA with biphase-bimodulation element.

process by separating the audio tones f_1 and f_2. Thus an audio signal proportional to the magnitude of the incident microwave components is generated. RMS to dc conversion allows the A/D converter of the data acquisition system to collect the required information for computation of the scattering parameters of the device under test (DUT).

III. Theoretical Development

A natural starting point when examining the operation of this new system is to consider the biphase-bimodulation element illustrated in Fig. 3.

Incident energy from the microwave source is split via a 3 dB Wilkinson power splitter, and the emergent waves α_1 and α_2 are modulated at two discrete audio frequencies by p-i-n diode modulators. The two audio tones modulate the microwave carrier in a specific manner; this is explained in Appendix I. It is required that the audio frequencies f_1 and f_2 not exhibit a multiple relationship, i.e., $m \cdot f_1 \neq n \cdot f_2$ $(m, n = 1, 2, \cdots)$ and not be adjacent in the spectral domain so that high-Q audio filters cannot separate them. The emergent waves from the modulators may be expressed as

$$\alpha_1 = \alpha_1|_{f_1} \tag{1a}$$

$$\alpha_2 = \alpha_2|_{f_2}. \tag{1b}$$

The nomenclature $|_{f_i}$ refers to a microwave carrier labeled by the audio tone f_i. The emergent waves from the modulators feed the isolated ports 1 and 2 of a broad-band quadrature coupler. This results in two emergent waves from the coupled ports. Due to the properties of the quadrature coupler, the emergent microwave carrier at ports 3 and 4 consists of two components. Considering

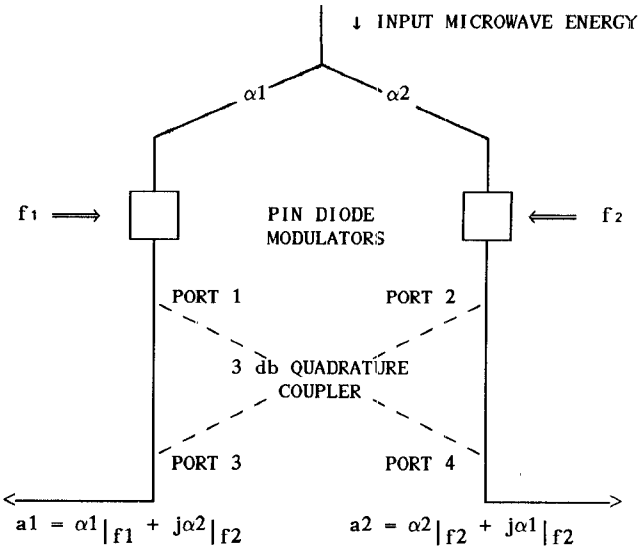

Fig. 3. The biphase-bimodulation element.

port 3, the emergent carrier consists of a carrier component from port 1 experiencing a 0° phase shift and labeled by the audio tone f_1 and a carrier component incident from port 2 experiencing a 90° phase shift and labeled by the audio tone f_2. The converse is true for the emergent wave from port 4; that is, the microwave carrier component experiencing a 90° phase shift is now labeled by the audio tone f_1 and the microwave carrier component experiencing a 0° phase shift is now labeled by the audio tone f_2.

Suppressing the coupling coefficient of the coupler, the emergent wave from port 3 may be expressed as

$$a_1 = \alpha_1|_{f_1} + j \cdot \alpha_2|_{f_2} \tag{2a}$$

and the emergent microwave carrier from port 4 may be expressed as

$$a_2 = \alpha_2|_{f_2} + j \cdot \alpha_1|_{f_1}. \tag{2b}$$

In practice the quadrature coupler will not be perfect and a phase shift of 90° will not occur. The departure from the quadrature condition is then denoted by some complex values R_1 and R_2. Thus equations (2) may be expressed as

$$a_1 = \alpha_1|_{f_1} + R_1 \cdot \alpha_2|_{f_2} \tag{3a}$$

$$a_2 = \alpha_2|_{f_2} + R_2 \cdot \alpha_1|_{f_1}. \tag{3b}$$

It must be understood that the audio tones $|_{f_1}$ and $|_{f_2}$ act as labels by which individual microwave carrier components are identified. It must also be stressed that the differential phase shift incurred by using the quadrature coupler takes effect upon the microwave carrier components.

It is instructive at this point to draw a comparison with existing dual six-port systems which incorporate a mechanical phase shifter. Two positions of the phase shifter are the minimum required for full S-parameter characterization of the DUT. In the biphase-bimodulation system, two phase states coexist owing to the properties of the quadrature coupler. These two states are distinguished by the audio tones which act as identification labels.

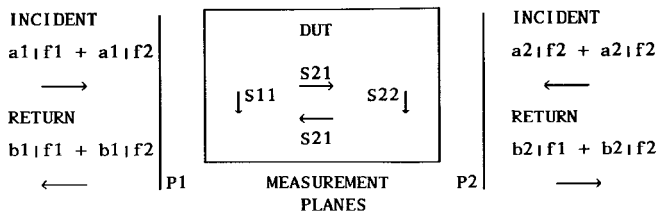

Fig. 4. Incident and emergent waves at DUT measurement planes.

IV. Network Analyzer Operation

Referring to Fig. 2. The emergent energy from the biphase-bimodulation element is fed to the six-ports. The combined carrier components from port 3 feed the LHS six-port and those from port 4 feed the RHS six-port. Examination of Fig. 4 identifies the incident waves upon the device under test. These are as follows:

At measurement plane P_1,

$$a_1 = \alpha_1|_{f_1} + R_1 \cdot \alpha_2|_{f_2}. \tag{4a}$$

At measurement plane P_2,

$$a_2 = \alpha_2|_{f_2} + R_2 \cdot \alpha_1. \tag{4b}$$

It may be noticed that these equations are similar in form to equations (3). Since the six-port introduces equal phase delay for all microwave carrier components of the same wavelength, the phase relationship between carrier components is maintained. The return waves at the measurement planes P_1 and P_2 may then be expressed as follows:

At measurement plane P_1,

$$b_1 = \beta_1|_{f_1} + \beta_2|_{f_2}. \tag{5a}$$

At measurement plane P_2,

$$b_2 = \beta_2|_{f_2} + \beta_1|_{f_1}. \tag{5b}$$

No implicit phase relationship can be deduced between the microwave carrier components; this is dependent upon the characteristics of the device under test.

The ratio of an emergent to incident microwave carrier is known as the reflection coefficient Γ. This is defined with respect to a measurement plane as

$$\Gamma = \frac{\text{emergent}}{\text{incident}} = \frac{b}{a}. \tag{6}$$

Existing single and dual six-port network analyzers are calibrated so that the reflection coefficient Γ may be directly evaluated.

Due to the audio labeling, two complex quantities at each measurement plane may be defined:

At the left-hand measurement plane P_1,

$$\Gamma_{11} = \left.\frac{b_1}{a_1}\right|_{f_1} \tag{7a}$$

$$\Gamma_{12} = \left.\frac{b_1}{a_1}\right|_{f_2}. \tag{7b}$$

At the right-hand measurement plane P_2,

$$\Gamma_{21} = \left.\frac{b_2}{a_2}\right|_{f_1} \tag{7c}$$

$$\Gamma_{22} = \left.\frac{b_2}{a_2}\right|_{f_2}. \tag{7d}$$

The nomenclature $|_{f_t}$ corresponds to the ratio of emergent to incident microwave carrier components labeled by the audio tone f_t. These quantities are regarded as pseudo reflection coefficients.

Central to the operation of this technique is the assumption that the microwave device under test obeys the following criteria:

$$\text{DUT performance parameter}\Big|_{\text{microwave frequency} \pm \text{audio frequency } f_1} = \text{DUT performance parameter}\Big|_{\text{microwave frequency} \pm \text{audio frequency } f_2}.$$

This assumption is valid for most measurement applications since $f_1 + f_2 \leqslant 20$ kHz and the microwave carrier $\geqslant 2$ GHz. As the technique is extended toward millimeter waves the assumption becomes stronger.

V. S-Parameter Evaluation

Fig. 4 depicts the incident and emergent waves at the two measurement planes P_1 and P_2. For any two-port network the relationship between the waves is expressed by the standard scattering matrix:

$$\begin{bmatrix} b_1 \\ b_2 \end{bmatrix} = \begin{bmatrix} S_{11} & S_{12} \\ S_{21} & S_{22} \end{bmatrix} \begin{bmatrix} a_1 \\ a_2 \end{bmatrix}. \tag{8}$$

For the situation portrayed in Fig. 4, (8) is rewritten, injecting the labeled components of the incident and emergent waves as

$$\begin{bmatrix} b_1|f_1 + b_1|f_2 \\ b_2|f_1 + b_2|f_2 \end{bmatrix} = \begin{bmatrix} S_{11} & S_{12} \\ S_{21} & S_{22} \end{bmatrix} \begin{bmatrix} a_1|f_1 + a_1|f_2 \\ a_2|f_1 + a_2|f_2 \end{bmatrix}. \tag{9}$$

Expanding yields

$$b_1|f_1 + b_1|f_2 = S_{11} \cdot (a_1|f_1 + a_1|f_2) + S_{12} \cdot (a_2|f_1 + a_2|f_2) \tag{10a}$$

$$b_2|f_1 + b_2|f_2 = S_{21} \cdot (a_1|f_1 + a_1|f_2) + S_{22} \cdot (a_2|f_1 + a_2|f_2). \tag{10b}$$

Carrier components labeled by f_1 and f_2 are independent; equations (10) may be separated:

$$b_1|f_1 = S_{11} \cdot a_1|f_1 + S_{12} \cdot a_2|f_1 \tag{11a}$$

$$b_1|f_2 = S_{11} \cdot a_1|f_2 + S_{12} \cdot a_2|f_2 \tag{11b}$$

$$b_2|f_1 = S_{21} \cdot a_2|f_1 + S_{22} \cdot a_2|f_1 \tag{11c}$$

$$b_2|f_2 = S_{21} \cdot a_2|f_2 + S_{22} \cdot a_2|f_2. \tag{11d}$$

Rearranging (2)–(11) to reform the pseudo reflection coef-

ficients Γ_{ij} yields

$$\Gamma_{11}=\left.\frac{b_1}{a_1}\right|_{f_1}=\left.S_{11}+S_{12}\cdot\frac{a_2}{a_1}\right|_{f_1} \tag{12a}$$

$$\Gamma_{12}=\left.\frac{b_1}{a_1}\right|_{f_2}=\left.S_{11}+S_{12}\cdot\frac{a_2}{a_2}\right|_{f_2} \tag{12b}$$

$$\Gamma_{21}=\left.\frac{b_2}{a_2}\right|_{f_1}=\left.S_{22}+S_{21}\cdot\frac{a_1}{a_2}\right|_{f_1} \tag{12c}$$

$$\Gamma_{22}=\left.\frac{b_2}{a_2}\right|_{f_2}=\left.S_{22}+S_{21}\cdot\frac{a_1}{a_2}\right|_{f_2}. \tag{12d}$$

Examination of the biphase-bimodulation element reveals that, ideally,

$$\left.\frac{a_2}{a_1}\right|_{f_1}=j \qquad \left.\frac{a_2}{a_1}\right|_{f_2}=1/j. \tag{13}$$

However, the ratio $a_2/a_1|_{f_i}$ is not only an instrumental parameter of the biphase-bimodulation element, it is also dependent upon the characteristics of the device under test. The precise relationship has been shown by Hoer [2] and Luff [5] to be of the form

$$\frac{a_2}{a_1}=\frac{\gamma\Gamma_1+\beta}{\delta\Gamma_2+1}. \tag{14}$$

For completeness, (14) is derived in Appendix II. For the biphase-bimodulation system two such relationships exist:

$$\left.\frac{a_2}{a_1}\right|_{f_1}=\frac{\gamma_1\Gamma_{11}+\beta_1}{\delta_1\Gamma_{21}+1} \tag{15a}$$

$$\left.\frac{a_2}{a_1}\right|_{f_2}=\frac{\gamma_2\Gamma_{12}+\beta_2}{\delta_2\Gamma_{22}+1} \tag{15b}$$

where the γ_i, β_i, and δ_i are instrumental parameters of the network analyzer, determined during the course of calibration. Equations (12) may now be augmented to form

$$\Gamma_{11}=\left.\frac{b_1}{a_1}\right|_{f_1}=\left.S_{11}+S_{12}\cdot\frac{\gamma_1\Gamma_{11}+\beta_1}{\delta_1\Gamma_{21}+1}\right|_{f_1} \tag{16a}$$

$$\Gamma_{12}=\left.\frac{b_1}{a_1}\right|_{f_2}=\left.S_{11}+S_{12}\cdot\frac{\gamma_2\Gamma_{12}+\beta_2}{\delta_2\Gamma_{22}+1}\right|_{f_2} \tag{16b}$$

$$\Gamma_{21}=\left.\frac{b_2}{a_2}\right|_{f_1}=S_{22}+S_{21}\cdot\left[\left.\frac{\gamma_1\Gamma_{11}+\beta_1}{\delta_1\Gamma_{21}+1}\right|_{f_1}\right]^{-1} \tag{16c}$$

$$\Gamma_{22}=\left.\frac{b_2}{a_2}\right|_{f_2}=S_{22}+S_{21}\cdot\left[\left.\frac{\gamma_2\Gamma_{12}+\beta_2}{\delta_2\Gamma_{22}+1}\right|_{f_2}\right]^{-1}. \tag{16d}$$

In the above equations Γ_{ij} are found from the measurement process, and γ_i, δ_i, and β_i are known instrumental constants. The scattering parameters of the device under test are evaluated by simple algebraic manipulation of equations (16). However before measurement, the network analyzer must be characterized and this is the subject of calibration.

VI. Calibration

Calibration proceeds in two steps. First each six-port is characterized so that each pseudo reflection coefficient Γ_{ij} may be evaluated. The second step is to determine the instrumental constants γ_i, β_i, and δ_i of equations (15).

If a six-port is correctly characterized, then the ratio of emergent to incident waves at the measurement plane may be evaluated [1] via

$$\Gamma=\frac{b}{a}=\frac{\sum_{i=1,3}^{6}(C_i+jS_i)\cdot P_i}{\sum_{i=1,3}^{6}B_i\cdot P_i}. \tag{17}$$

Here the C_i, S_i, and B_i are instrumental parameters, arising from the physical construction of the six-port junction, and the P_i represent the observed power readings at the detector ports. For our dual six-port system, four pseudo reflection coefficients Γ_{ij} are defined, and so four equations of type (17) are formed:

$$\Gamma_{11}=\left.\frac{b_1}{a_1}\right|_{f_1}=\left.\frac{\sum_{i=1,3}^{6}(C_i+jS_i)\cdot P_i}{\sum_{i=1,3}^{6}B_i\cdot P_i}\right|_{f_1} \tag{18a}$$

$$\Gamma_{12}=\left.\frac{b_1}{a_1}\right|_{f_2}=\left.\frac{\sum_{i=1,3}^{6}(C_i+jS_i)\cdot P_i}{\sum_{i=1,3}^{6}B_i\cdot P_i}\right|_{f_2} \tag{18b}$$

$$\Gamma_{21}=\left.\frac{b_2}{a_2}\right|_{f_1}=\left.\frac{\sum_{i=1,3}^{6}(C_i+jS_i)\cdot P_i}{\sum_{i=1,3}^{6}B_i\cdot P_i}\right|_{f_1} \tag{18c}$$

$$\Gamma_{22}=\left.\frac{b_2}{a_2}\right|_{f_2}=\left.\frac{\sum_{i=1,3}^{6}(C_i+jS_i)\cdot P_i}{\sum_{i=1,3}^{6}B_i\cdot P_i}\right|_{f_2}. \tag{18d}$$

Calibration characterizes the C_i, S_i, and B_i of equations (18). This is achieved by employing a technique developed by Judah [6]. The method requires a total of five standards, consisting of four offset shorts and a matched load.

Stage two requires the evaluation of γ_i, β_i, and δ_i the instrumental parameters of equations (15). Since each six-port is calibrated, and all four pseudo reflection coefficients Γ_{ij} can be correctly measured. Equations (16a), (16d) may be employed to evaluate the remaining instrumental parameters.

In this process a good air line is used as the calibrating standard. It is assumed the air line is nearly perfect, with characteristics $S_{11}=S_{22}=0$ and $S_{12}=S_{21}=e^{-j\theta}$. The air

line is connected between the two measurement planes and adjusted to three phase positions. At the position, each of the four pseudo reflection coefficients Γ_{ij} are recorded. For the air line, (16a) reduces to

$$\Gamma_{11} = e^{-j\theta} \cdot \frac{\gamma_1 \cdot \Gamma_{11} + \beta_1}{\delta_1 \cdot \Gamma_{21} + 1}. \quad (19)$$

Algebraic manipulation of (19) yields

$$\Gamma_{11} + \Gamma_{11} \cdot \Gamma_{21} \cdot \delta_1 - \Gamma_{11} \cdot e^{-j\theta} \cdot \gamma_1 - e^{-j\theta} \cdot \beta_1 = 0. \quad (20)$$

Three positions of the air line generate three equations of type (20) and these are solved simultaneously to evaluate γ_1, β_1, and δ_1. An identical procedure is followed for the parameters of (16b). Calibration is now complete.

VII. Experimental Prototype and Experimental Results

To test this technique, a prototype DSPANA incorporating a biphase-bimodulation element operating at 2 GHz was constructed. The six-port junctions consist of a Riblet [7] five-port ring and a 3 dB quadrature coupler. The biphase-bimodulation element was manufactured as one device, utilizing surface mount technology for the modulator p-i-n diodes and a Wilkinson power splitter. The audio tones were set at $f_1 = 800$ Hz and $f_2 = 2000$ Hz with an overall switching rate of 12 kHz. The detectors are HP11664A Schottky barrier diodes augmented by active high-Q audio filters. The ac output of each filter feeds an RMS to dc converter; this dc level corresponds to the magnitude of the incident microwave carrier and is recorded by the data acquisition system.

Fig. 5 depicts the performance for reflect and thru measurement. The device under test consists of nominal pads, in series with reflect and thru constant-impedance air lines. Each air line is stepped through a complete electrical wavelength. Table I compares theoretical and actual S-parameter measurements for both reflect and thru air line loads. This assumes that the standards are perfect. The overall accuracy of the system operating with non-characterized HP11664A diode detectors is estimated at better than ± 0.02 for a Mod 1 load (nominal reflection coefficient of unity). It is pertinent to mention that two known error mechanisms manifest themselves within these results.

The major error mechanism is that of detector nonlinearity, typically 1 percent nonlinearity over the dynamic range. Upon characterization of each detector, an increase in accuracy would be expected that is comparable to that reported by Hoer [8] (accuracy of ± 0.001 in a Mod 1 load). The second error mechanism is crosstalk between the audio filters. This corrupts the true power reading associated with each audio frequency label. Preliminary calculations indicate that a crosstalk factor of -30 dB will cause an estimated error of ± 0.01 in a Mod 1 load. The prototype filters in this system have an integrity better than -50 dB with respect to crosstalk. As such this error mechanism is considered to be insignificant at this stage.

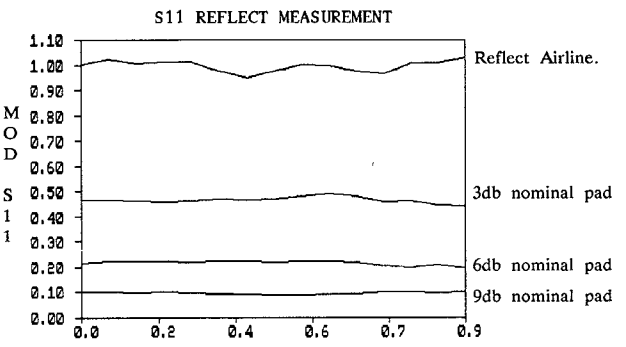

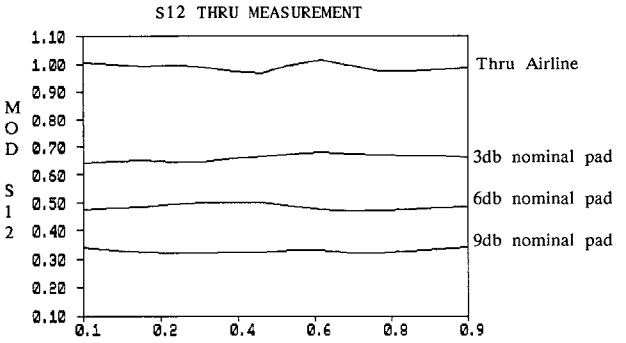

Fig. 5. Reflect and thru performance.

TABLE I
Measurement Performance

Reflect Performance.

	|S11| Phase |S22| Phase	|S12| Phase |S21| Phase
Theoretical	1.000 00.00	0.000 0.000
Actual	1.003 -00.22 0.997 -04.89	0.003 - - - 0.005 - - -
Theoretical	1.000 90.00	0.000 0.000
Actual	0.999 89.90 0.982 86.14	0.003 - - - 0.008 - - -
Theoretical	1.000 180.00	0.000 0.000
Actual	0.986 180.34 0.992 177.62	0.002 - - - 0.004 - - -

Thru Performance.

	|S11| Phase |S22| Phase	|S12| Phase |S21| Phase
Theoretical	0.000 00.00	1.000 00.00
Actual	0.013 - - - 0.015 - - -	0.993 -00.18 1.005 00.03
Theoretical	0.000 00.00	1.000 120.00
Actual	0.016 - - - 0.038 - - -	0.997 119.12 0.992 120.36
Theoretical	0.000 00.00	1.000 240.00
Actual	0.001 - - - 0.009 - - -	1.000 240.11 1.004 239.82

System speed is excellent, requiring only 50 ms for data acquisition and computation of all four S parameters in magnitude and phase. A major limitation to speed is the slow 4 MHz computer and the multiplexed analog to digital converter used for data acquisition.

VIII. Conclusions and Points of Application

This paper presents experimental validation of the biphase-bimodulation technique when applied to a dual six-port network analyzer. The technique allows construction of a dual six-port automatic network analyzer which exhibits some positive advantages over conventional designs:

1) No computer synchronization with mechanical phase shifters and the data acquisition system is required.
2) Improved sensitivity and elimination of drift are a consequence of ac modulation.
3) The ability to perform quasi-real-time evaluation of scattering parameters in a swept frequency system.

Appendix I

The audio tones f_1 and f_2 modulate the microwave carrier in specific manner. The Schottky barrier diodes employed as detectors are square law devices whose output is directly proportional to the square of the applied incident field:

$$\text{detector output} = (\text{incident field})^2. \tag{A1}$$

If two AM carriers a and b which correspond to the microwave carrier components labeled by the tones f_1 and f_2 are coincident, then the detector output is

$$\text{detector output} = (a+b)^2 = a^2 + b^2 + 2ab. \tag{A2}$$

The term $2ab$ is an intermodulation product; such products are undesirable since this will manifest itself as a deviation from a true square law response.

The problem of coincident carriers is overcome by applying the modulation tones f_1 and f_2 to the p-i-n diode modulators in the following manner. Referring to Fig. 3, when audio tone f_1 is applied, the opposing modulator corresponding to the audio tone f_2 is driven hard off. This allows a unique microwave carrier labeled f_1 to propagate. The role is then reversed with audio tone f_2 applied and the opposing modulator driven hard off, again allowing a unique carrier labeled f_2 to propagate. The switching speed between the two states is chosen to be much higher than that of f_1 and f_2, such that the Nyquist criterion is satisfied. Due to the high speed of switching, this process becomes latent, and the filters employed within the detection system "apparently" observe a continuous waveform rather than the actual sampled waveform.

In practice $f_1 = 800$ Hz, $f_2 = 2000$ Hz, and the switching rate is 12 kHz. These values are not critical, the only criteria for selection being that $n \cdot f_1 \neq m \cdot f_2$ (m, n are integers) and that the switching rate be high enough to satisfy the minimum 2× Nyquist condition.

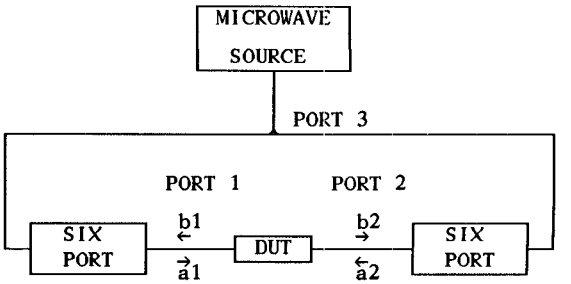

Fig. 6. The three-port system.

Appendix II
The Six to Three Six-Port Reduction

The complex ratio $R = a_2/a_1$ is not constant, but is dependent upon the device under test. Both Hoer [2] and Luff *et al.* [5] have reported this, and several techniques have been developed [9], [10] which evaluate this ratio.

The characterization of $R = a_2/a_1$ is found by reducing the network analyzer to a three-port as shown in Fig. 6. Consider a linear two-port device under test connected between the measurement planes P_1 and P_2. This is analyzed in terms of the S parameters of the device under test and the incident and emergent waves:

$$b = s \cdot a \tag{A3a}$$

$$b_1 = s_{11} \cdot a_1 + s_{12} \cdot a_2 \tag{A3b}$$

$$b_2 = s_{21} \cdot a_1 + S_{22} \cdot a_2. \tag{A3c}$$

Defining

$$R = a_2/a_1 \tag{A4}$$

and dividing (A3b) by a_2 and (A3c) by a_1 gives

$$\Gamma_1 = s_{11} + s_{12} \cdot R \tag{A5a}$$

$$\Gamma_2 = s_{21} + s_{22}/R \tag{A5b}$$

where $\Gamma_1 = b_1/a_1$ and $\Gamma_2 = b_2/a_2$.

The parameters Γ_1 and Γ_2 are the pseudo reflection coefficients, measured at the DUT planes of the six-ports. The complex ratio R is the ratio of the incident waves at the two ports of the device under test.

The six-port measurement ports are labeled 1 and 2; the excitation port forms port 3 of the network, which exhibits scattering parameters S_{ij} (not to be confused with the s_{ij} scattering parameters of the device under test.)

The notation of a_i and b_i, i.e., the incident and emergent waves upon the DUT, is retained. The scattering equations can now be written for a_1 and a_2 as

$$a_1 = S_{11} \cdot b_1 + S_{12} \cdot b_2 + S_{13} \cdot A \tag{A6a}$$

$$a_2 = S_{21} \cdot b_1 + S_{22} \cdot b_2 + S_{23} \cdot A \tag{A6b}$$

with

$$A = (a_1 - S_{11} \cdot b_1 - S_{12} \cdot B_2)/S_{13}$$
$$= (a_2 - S_{21} \cdot b_1 - S_{22} \cdot b_2)/S_{23} \tag{A7}$$

where A is the excitation signal from the microwave source. Dividing by a_1 and rearranging gives the desired expres-

sion for the complex ratio R:

$$R = R_0 \frac{(1 - S_{11}\cdot\Gamma_1 + S_{21}/R_0\cdot\Gamma_1)}{(1 - S_{22}\cdot\Gamma_2 + S_{12}\cdot R_0\cdot\Gamma_2)} \tag{A8}$$

where $R_0 = S_{23}/S_{13}$. It is instructive to note that R_0 is that value of R which occurs when both reflectometers are terminated with a matched load. Equation (A8) is of the form

$$R = \frac{\gamma\cdot\Gamma_1 + \delta}{\beta\cdot\Gamma_2 + 1} \tag{A9}$$

as referenced in the text.

References

[1] G. F. Engen, "The six-port reflectometer: An alternative network analyser," *IEEE Trans. Microwave Theory Tech.*, vol. MTT-25, pp. 1075–1079, Dec. 1977.

[2] C. A. Hoer, "A network analyser incorporating two six-ports," *IEEE Trans. Microwave Theory Tech.*, vol. MTT-25, pp. 1070–1074, Dec. 1977.

[3] C. A. Hoer, "Performance of a dual six-port automatic network analyser," *IEEE Trans. Microwave Theory Tech.*, vol. MTT-27, pp. 993–998, Dec. 1979.

[4] S. K. Judah and A. S. Wright, "A second generation dual six-port network analyser," *IEEE Trans. Microwave Theory Tech.*, in *IEEE MTT-S Int. Microwave Symp. Dig.*, May 1988, pp. 295–296.

[5] G. F. Luff, P. J. Probert, and J. E. Carroll, "New calibration method for a 7-port reflectometer," *Proc. Inst. Elec. Eng.*, vol. 134, pt. A, no. 7, pp. 595–600, July 1987.

[6] S. K. Judah, "Calibration of multiport reflectometers," *Proc. Inst. Elec. Eng.*, pt. H, vol. 132, no. 7, pp. 46–470, Dec. 1985.

[7] M. D. Judd and S. K. Judah, "Direct Synthesis of the matched symmetrical five port junction from the scattering matrix," *Proc. Inst. Elec. Eng.*, pt. H, vol. 123, no. 2, pp. 95–98, Apr. 1986.

[8] J. R. Juroshek and C. A. Hoer, "A dual six-port network analyser using diode detectors," *IEEE Trans. Microwave Theory Tech.*, vol. MTT-32, pp. 51–57, Jan. 1984.

[9] G. F. Engen and C. A. Hoer, "Thru reflect line: An improved technique for calibrating the dual six port automatic network analyser," *IEEE Trans. Microwave Theory Tech.*, vol. MTT-27, pp. 987–993, Dec. 1979.

[10] Shi-He Li and R. G. Bosisio, "The automatic measurement of N-port microwave junctions by means of the six-port technique," *IEEE Trans. Instrum. Meas.*, vol. IM-31, pp. 40–43, Mar. 1982.

[11] A. L. Cullen, S. K. Judah, and F. Nikravesh, "Impedance measurement using a six-port directional coupler," *Proc. Inst. Elec. Eng.*, vol. 127, pt. H, no. 2, pp. 93–98, Apr. 1980.

[12] H. M. Cronson and L. Susman, "A dual six-port automatic network analyser," *IEEE Trans. Microwave Theory Tech.*, vol. MTT-29, pp. 372–379, Apr. 1981.

[13] G. P. Riblet and E. R. B. Hanson, "Aspects of the calibration of a single six-port using a load and offset reflection standards," *IEEE Trans. Microwave Theory Tech.*, vol. MTT-30, pp. 2120–2125, Dec. 1982.

[14] G. P. Riblet and E. R. Bertil Hanson, "The use of a symmetrical five-port junction to make six-port measurements," *IEEE Trans. Microwave Theory Tech.*, vol. MTT-29, pp. 151–153, Feb. 1981.

Sunil R. Judah (M'85) was born in 1945. He received the B.Eng. (hons) from Jabalpur University, India, in 1966, the M.Sc. degree from University College London, England, in 1969, and the Ph.D. degree, also from University College London, in 1975.

At present he is a lecturer in microwave theory and techniques in the Department of Electronic Engineering, University of Hull, Hull, U.K. His research interests include microwave metrology and passive component design, in particular patch antennas.

Andrew S. Wright was born in 1964 in Bishop's Stortford, Hertfordshire, England, He received the B.Sc. (hons) in 1986 and the Dip.Eng. in 1986, both from Hull University Hull, U.K. He is currently pursuing the Ph.D. degree in microwave metrology at Hull University.